ISA Transactions 63 (2016) 315–327

Contents lists available at ScienceDirect

ISA Transactions

journal homepage: www.elsevier.com/locate/isatrans

Research Article

Predictive optimized adaptive PSS in a single machine infinite bus

Freddy Milla [a,b,*], Manuel A. Duarte-Mermoud [a,b]

[a] Department of Electrical Engineering, University of Chile, Av. Tupper 2007, Santiago de Chile, Chile
[b] Advanced Mining Technology Center, Av. Tupper 2007, Santiago de Chile, Chile

ARTICLE INFO

Article history:
Received 28 October 2014
Received in revised form
4 February 2016
Accepted 27 February 2016
Available online 24 March 2016
This paper was recommended for publication by Dr. Q.-G. Wang

Keywords:
Predictive Optimized Adaptive PSS
PSS
MPC
Electric power system
SMIB
PSO

ABSTRACT

Power System Stabilizer (PSS) devices are responsible for providing a damping torque component to generators for reducing fluctuations in the system caused by small perturbations. A Predictive Optimized Adaptive PSS (POA-PSS) to improve the oscillations in a Single Machine Infinite Bus (SMIB) power system is discussed in this paper. POA-PSS provides the optimal design parameters for the classic PSS using an optimization predictive algorithm, which adapts to changes in the inputs of the system. This approach is part of small signal stability analysis, which uses equations in an incremental form around an operating point. Simulation studies on the SMIB power system illustrate that the proposed POA-PSS approach has better performance than the classical PSS. In addition, the effort in the control action of the POA-PSS is much less than that of other approaches considered for comparison.

1. Introduction

The ability of the machines of an electric power system to remain in synchronism corresponds to the rotor angle stability. This stability can be broken either by an aperiodic deflection angle, because of a lack of synchronizing torque, or oscillatory instability problems that arise from the lack of damping torque. Power System Stabilizer (PSS) devices are responsible for providing a damping torque component to generators for the purpose of reduced fluctuations in the system caused by small perturbations. Information on the optimal tuning of these devices can be found in [1–4].

The enhancement of power system stability by optimal tuning and placement of PSS using evolutionary algorithms (Particle Swarm Optimization – PSO) is presented in [5]. In this approach, Matlab and a program for simulation of electric power systems (DigSILENT) are employed and linked together in a genuine automatic data exchange procedure. Consequently, the test system and the controllers are modeled in DigSILENT, and the PSO algorithm is implemented in Matlab. For evaluating the particles evolution throughout the searching process, an eigenvalue-based multi-objective function is used. The performance of the proposed PSO based PSS test system in damping power system oscillations is proved through eigenvalue analysis and time-domain simulations. In [13], chaotic ant swarm optimization (CASO) is utilized to tune the parameters of both single input and dual-input power system stabilizers (PSSs). This algorithm explores the chaotic and self-organization behavior of ants in the foraging process. While comparing CASO with either particle swarm optimization or genetic algorithm, it is revealed that CASO is more effective than the others in finding the optimal transient performance of a PSS and an automatic voltage regulator equipped single machine-infinite-bus system. Conventional PSS and the three dual input IEEE PSSs (PSS2B, PSS3B, and PSS4B) are optimally tuned to obtain the optimal transient performances. It is shown that the transient performance of the dual-input PSS is better than a single-input PSS. Further, whether PSS3B offers superior transient performance among dual-input PSSs is explored. The Takagi Sugeno fuzzy logic (SFL) based approach is adopted for on-line, off-nominal operating conditions. For real time measurements of system operating conditions, SFL adaptively and very quickly yields on-line, off-nominal optimal stabilizer variables.

According to [6] the tuning of PSS parameters for satisfactory power system response over a wide range of operating conditions requires an efficient robust optimization technique. The authors present a novel concept of integrating the Taguchi robust design principle with particle swarm optimization (PSO) for the PSS design.

* Corresponding author at: Department of Electrical Engineering, University of Chile, Av. Tupper 2007, Santiago de Chile, Chile. Tel.: +56 2 29784207; fax: +56 2 6720162.
E-mail addresses: fmilla@ing.uchile.cl (F. Milla), mduartem@tamarugo.cec.uchile.cl (M.A. Duarte-Mermoud).

http://dx.doi.org/10.1016/j.isatra.2016.02.018
0019-0578/

The objective is to build intrinsic robustness into the design of PSS over a wide range of power system operating conditions. The proposed approach employs signal to noise ratio and orthogonal array concepts of the Taguchi design to determine the robust optimal setting of PSS parameters using PSO. The robustness of the designed PSS is tested through the No-Way analysis of variance. Further, the effectiveness of the robust PSS is illustrated through time-domain simulations as it is applied to a single machine infinite bus system under a wide range of loading conditions. Ref. [17] describes a technique to improve the damping of inter-area modes in power systems. This technique consists of coordinate power system stabilizers (PSSs), in order for the system to exhibit a good performance under different operating conditions, and it is based on the evaluation of the closed-loop characteristic polynomial on a frequency interval. Analysis of controllability, observability and participation factors is employed in the location of the PSSs. Results on an actual electrical grid are presented showing the applicability of the proposed technique.

Among the online optimization techniques for improving the system performance for damping power oscillations in electric power systems, we can mention those based on Model Predictive Controller (MPC), whose mathematical basis can be found in [14,15]. Among the outstanding works, we can mention, the articles studying the integration of teams generators, Flexible AC Transmission Systems (FACTS) and High Voltage Direct Current (HVDC) Transmission System [7–12,18] where the approaches show the advantage of the MPC technique. In particular, [12] presents a framework for the development of discrete-time, nonlinear predictive controllers using thyristor-controlled-series-capacitors and phasor measurements of bus voltage magnitude and angle, for the stabilization and rapid damping of multi-machine power systems which are subjected to large disturbances. When the faults of concern are large, the nonlinear predictive controllers are used to return the power system state to a small region about the post-fault equilibrium. In this region, linear controllers provide local asymptotic stability and rapid damping. Simulation results are provided on a sample four-machine power system.

In [20] the ability of Predictive Control in coordinate design of two PSSs and a supplementary controller for Static Var Compensators (SVC) to damp the power system inter-area oscillation is investigated. For this, the parameters of the PSSs and the supplementary controller are determined simultaneously by Generalized Predictive Control (GPC). In [21] a novel real-time predictive control technique to damp dominant inter-area oscillation modes in power systems is presented. In this work, we design a centralized MPC to provide supplementary control to these conventional PSSs based on a Selective Discrete Fourier Transform (SDFT) approach. The SDFT extracts the energies associated with the inter-area frequency components in the output spectrum of the system and uses this information to construct a weighting matrix Q. The MPC is then formulated as a quadratic minimization of the outputs using Q, resulting in damping only the inter-area modes of interest. In [22] the power system stabilizer based on neural predictive control for improving power system dynamic performance over a wide range of operating conditions is investigated. In this study a design and application of the neural network model predictive controller (NN-MPC) on a simple power system composed of a synchronous generator connected to an infinite bus through a transmission line is proposed. In [23] a robust control framework for power system stabilizer to improve system dynamic performance based on MPC is proposed. The effectiveness of the proposed power system stabilizer is validated by a simple power system composed of a synchronous generator connected to an infinite bus through a transmission line. However, this paper does not provide enough information to make comparisons. Finally, in [24] a Model Predictive Power Stabilizer Optimized (MPPS) optimized by PSO is presented and will be the basis of comparison for the present work.

This paper is organized as follows. In Section 2, the problem of the damping of the power oscillations is presented. In Section 3, a predictive optimized technique by means of online optimization of the parameters of a Conventional Power System Stabilizer (CPSS) and the design of a Predictive Optimized Adaptive PSS (POA-PSS) strategy are presented, as well as the mathematical and physical principles that support this work. In Section 4, the features of the damping strategies used for comparison, the features of the proposed design POA-PSS, and the evaluation parameters are presented. Finally, the results on the variation of the active power, reactive power and results compared with other studies are shown. In Section 5, some conclusions are provided.

2. Presentation of problem

Electric power systems are susceptible to becoming unstable due to the problems associated with the oscillation of the rotor of the synchronous generators. To damp these oscillations, the incorporation of a device in the excitation system of these machines is required. This device is the power system stabilizer (PSS). To provide damping, the PSS must insert an electric torque component in phase with the variation of the rotor speed; the input signal to the PSS is the frequency variation of the rotor.

In this work, a POA-PSS to improve the oscillations in a Single Machine Infinite Bus (SMIB) power system is considered. The classical SMIB is presented in Fig. 1.

In general, a linearized model of SMIB represents the dynamic behavior of an electric power system, which includes the electromechanical torque relationship between acceleration and the speed and angle deviations, the damping of the turbine, the synchronizing torque and flow dynamics generator [7].

The block diagram of the SMIB system with an Automatic Voltage Regulator (AVR) [17], thyristor high gain exciter, synchronous generator and PSS is shown in Fig. 2. The generator, including AVR, excitation system and transmission-circuit reactance, is represented by a two-axis, fourth order model. IEEE type ST1A model of the static excitation system is considered [17].

A CPSS has been widely used for enhancing overall stability of large power systems [3]. The CPSS fixed structure composed of a cascade connected lead–lag network with rotor speed deviation as input has made a great contribution to enhancing system stability. The CPSS considered here is the conventional lead–lag network with gain K_s, and lead–lag time constants T_1, T_2; and T_w is the washout time constant, used to washout DC signals, without which the steady-state changes in speed would modify the terminal voltage. The CPSS can be seen at the top of Fig. 2, where $\Delta\omega_r$, $\Delta\delta$ and $\Delta\psi_{fd}$ are speed deviation, rotor angle deviation and field flux deviation respectively. ΔE_{fd}, ΔT_e and ΔT_m represent field voltage deviation, electrical torque deviation and mechanical torque deviation, respectively. ΔV_s, ΔV_1, ΔV_2, ΔV_{ref} and ΔE_t represent CPSS voltage deviation, transducer voltage deviation, reference voltage deviation, internal CPSS voltage deviation and terminal voltage deviation respectively. $G_{ex}(s)$, is the transfer

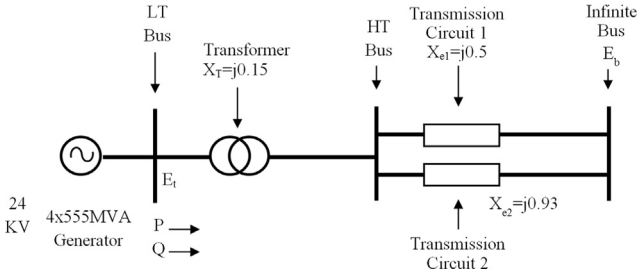

Fig. 1. Single-machine-infinite-bus test system.

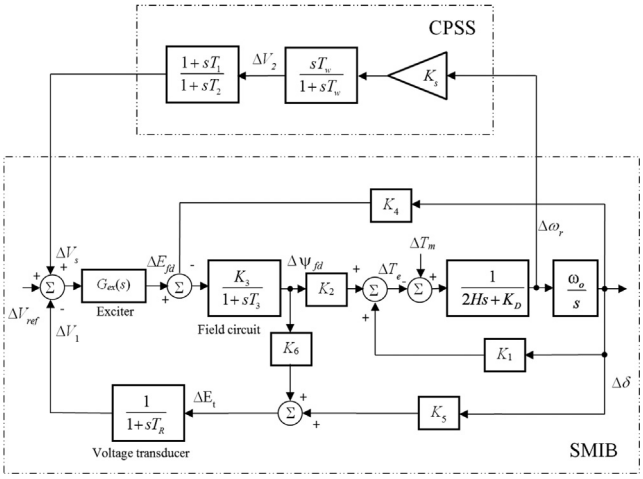

Fig. 2. Block diagram representation of SMIB system with AVR, thyristor high gain exciter, synchronous generator, and CPSS.

function of AVR and the exciter; for a thyristor exciter $G_{ex}(s) = K_A$. Finally, K_A, $K_1, \ldots, K_6$, H, K_D, T_3 and T_R are parameters of system [17], they are functions of active power P with the exception of H.

3. Predictive optimized technique

In this section, design CPSS and design POA-PSS strategy are presented and the mathematical and physical principles that support this work are introduced.

3.1. Online optimization of the parameters of a CPSS

A control technique that damps the oscillation modes in SMIB by means of online optimization of the parameters of a CPSS is proposed. The methodology for obtaining the parameters considers predicting the future behavior of a system through the explicit use of an SMIB system model. The generation of the optimal signal of the parameter is made through the minimization of an objective function, which penalizes the system state forcing convergence to the origin. Therefore, the variation of the angle of the rotor machine tends to zero, since it is one of the components of the state. This technique is based on the MPC algorithm [9], which is based, essentially, on the use of a finite slide horizon control, which involves the calculation of the control sequence for the whole horizon, but only the first control signal in the sequence is applied to the plant, and the process is repeated in the next sampling instant.

In Fig. 3, the simplified structure of the POA-PSS is presented where the control action can explain the following process: the first block updates the initial conditions of the discrete linear model of the SMIB, from the signals $\Delta\omega_r$, $\Delta\delta$, $\Delta\psi_{fd}$, ΔV_1, ΔV_2 and ΔV_s besides the active power signal P, each sampling interval $T_s = 0.3$[s], then in a next block, a prediction for N steps of the SMIB model is made. Finally in the last block, the optimal parameter vector $p^* = [K_s^* \; T_1^* \; T_2^*]'$ is generated as a solution of the optimization problem which considers the objective function J (in Section 3.1 more details are presented) (Fig. 4).

Note that within the variables that consider the CPSS, the washout time T_w was kept constant for simplicity, since this filter is defined for a fixed frequency range. Including this parameter in the optimization of the controller in a constrained operating range is proposed as a future work.

In this section, the design of the MPPS and the design of the optimizer CPSS for damping the oscillation modes in SMIB, including restrictions and optimization problem, are presented.

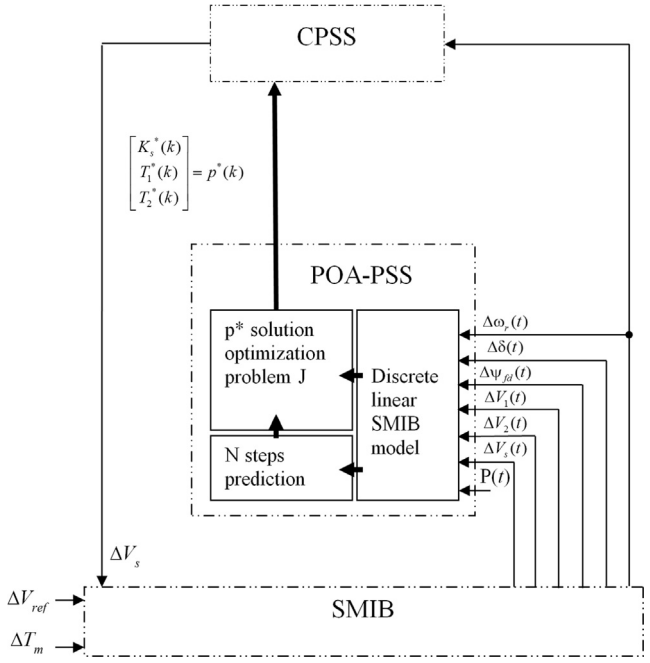

Fig. 3. Block diagram representation of SMIB system with AVR, thyristor high gain exciter, synchronous generator, and POA-PSS.

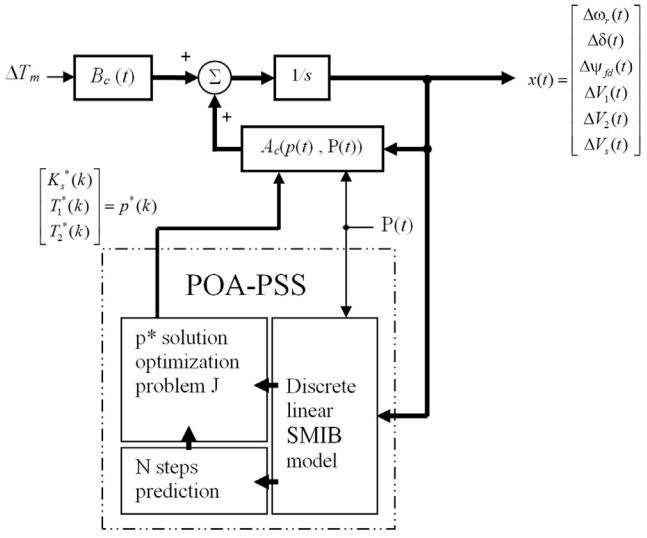

Fig. 4. SMIB linearized model with POA-PSS.

3.2. Design of the POA-PSS strategy

The mathematical foundations of the proposed POA-PSS control strategy are shown below.

In the mathematical form, the SMIB linear model of Fig. 2 can be represented as the dynamic system (1):

$$\begin{bmatrix} \Delta\dot{\omega}_r(t) \\ \Delta\dot{\delta}(t) \\ \Delta\dot{\Psi}_{fd}(t) \\ \Delta\dot{V}_1(t) \\ \Delta\dot{V}_2(t) \\ \Delta\dot{V}_s(t) \end{bmatrix} = \begin{bmatrix} a_{11} & a_{12} & a_{13} & 0 & 0 & 0 \\ a_{21} & 0 & 0 & 0 & 0 & 0 \\ 0 & a_{32} & a_{33} & a_{34} & 0 & a_{36} \\ 0 & a_{42} & a_{43} & a_{44} & 0 & 0 \\ a_{51} & a_{52} & a_{53} & 0 & a_{55} & 0 \\ a_{61} & a_{62} & a_{63} & 0 & a_{65} & a_{66} \end{bmatrix} \begin{bmatrix} \Delta\omega_r(t) \\ \Delta\delta(t) \\ \Delta\psi_{fd}(t) \\ \Delta V_1(t) \\ \Delta V_2(t) \\ \Delta V_s(t) \end{bmatrix}$$

$$+\begin{bmatrix} b_{11} \\ 0 \\ 0 \\ 0 \\ 0 \\ 0 \end{bmatrix} \Delta T_m(t) \tag{1}$$

where $a_{11}, a_{12}, a_{13}, a_{21}, a_{32}, a_{33}, a_{34}, a_{36}, a_{42}, a_{43}, a_{44}$ and b_{11} are parameters of SMIB [17]. Defining the state $x(t) = [\Delta\omega_r\ \Delta\delta\ \Delta\psi_{fd}\ \Delta V_1\ \Delta V_2\ \Delta V_s]$':

$$A_c = \begin{bmatrix} a_{11} & a_{12} & a_{13} & 0 & 0 & 0 \\ a_{21} & 0 & 0 & 0 & 0 & 0 \\ 0 & a_{32} & a_{33} & a_{34} & 0 & a_{36} \\ 0 & a_{42} & a_{43} & a_{44} & 0 & 0 \\ a_{51}(p(t)) & a_{52}(p(t)) & a_{53}(p(t)) & 0 & a_{55} & 0 \\ a_{61}(p(t)) & a_{62}(p(t)) & a_{63}(p(t)) & 0 & a_{65}(p(t)) & a_{66}(p(t)) \end{bmatrix}$$

and $B_c = \begin{bmatrix} b_{11} \\ 0 \\ 0 \\ 0 \\ 0 \\ 0 \end{bmatrix}$

where $a_{55} = 1/T_w$ and b_{11} are parameters of SMIB [17]. Parameters $a_{51}, a_{52}, a_{53}, a_{61}, a_{62}, a_{63}, a_{65}, a_{66}, a_{43}$ and a_{44} are functions of the parameter vector $p(t) = [K_s(t)\ \ T_1(t)\ \ T_2(t)]$' with $a_{51} = K_s a_{11}$, $a_{52} = K_s a_{12}$, $a_{53} = K_s a_{13}$, $a_{61} = a_{51} T_1/T_2$, $a_{62} = a_{52} T_1/T_2$, $a_{63} = a_{53} T_1/T_2$, $a_{65} = a_{55} T_1/T_2 + 1/T_2$, $a_{62} = -1/T_2$.

Fig. 5 shows a simplified model of the proposed control structure; it shows how POA-PSS delivers $p^*(t)$ optimal signal is based on the optimization of the objective function J, in (5), where the controlled variable $x(t)$ must converge to the origin. Fig. 5 shows the dependence of a matrix with parameter vector and the active power P.

3.2.1. SMIB linearized model

For continuous variables, the system (1) is described as:

$$\dot{x}(t) = A_c(p(t))x(t) + B_c(t)\Delta T_m(t) \tag{2}$$

The discrete model of the system with sampling time T_s is:

$$x(k+1) = A(p(k))_d x(k) + B_d(p(k))\Delta T_m(k) \tag{3}$$

with

$$A_d(p(k), T_s) = e^{A_c(p(k))T_s} \quad \text{and} \quad B_d(T_s) = (e^{A_c(p(k))T_s} - I)A_c(p(k))^{-1}B_c \tag{4}$$

ΔT_m can be predicted from a model based on real data. In our case ΔT_m is considered constant and equal to zero, because in the model, there is no primary or secondary frequency control.

3.2.2. Prediction as an optimization process

Damping the oscillation modes in SMIB by the MPC algorithm involves solving the optimization problem (5) to find the optimal set $\{p^*(k), \ldots, p^*(k+N_p-1)\}$ of control actions to N steps and apply the single signal $p^*(k)$ as control action:

$$\underset{p(k),\ldots,p(k-N+1)}{\text{minimize}} J(x(k), p(k)) = \sum_{i=1}^{N} x(k+i)^T M_a x(k+i) + \sum_{i=1}^{N} \Delta p(k+i-1)^T M_b \Delta p(k+i-1)$$

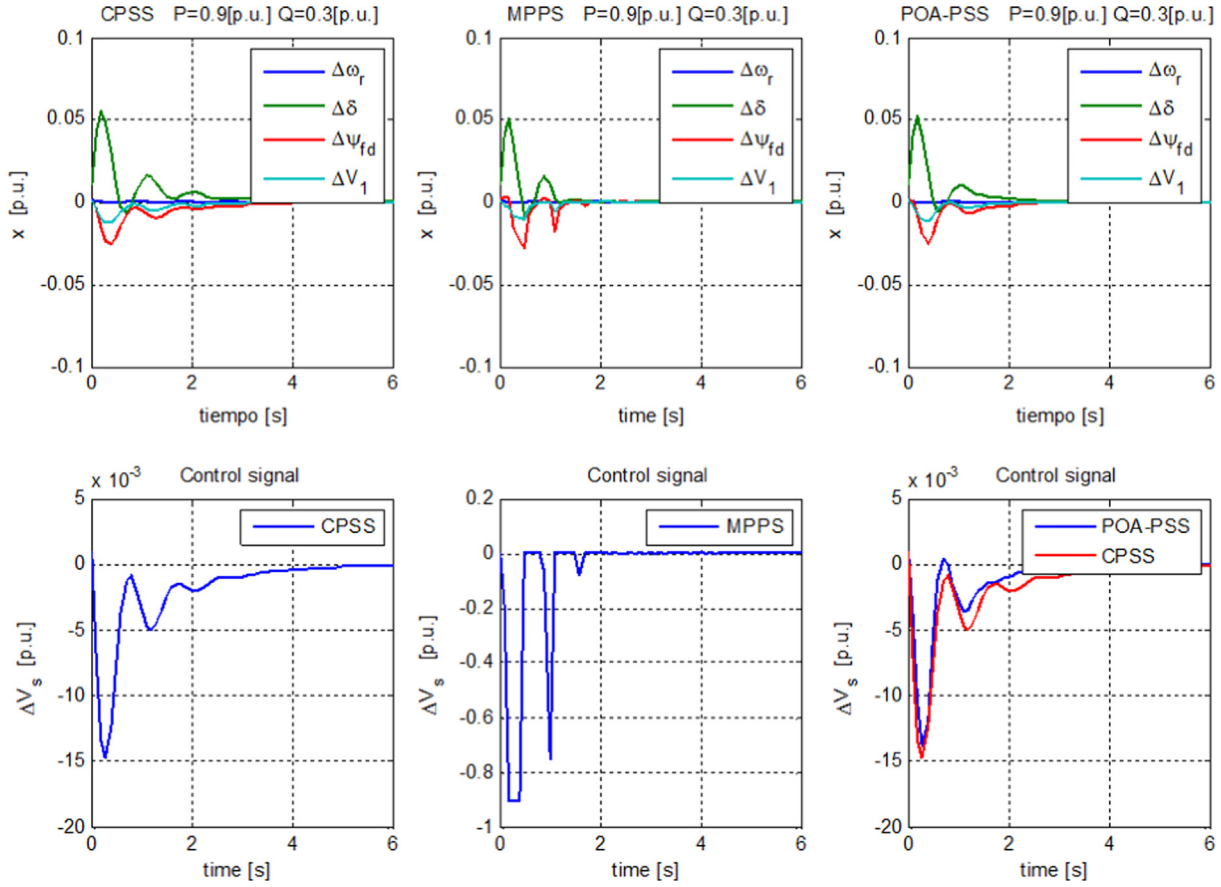

Fig. 5. State and control signal, two circuit connected, P=0.9 pu and Q=0.3 pu.

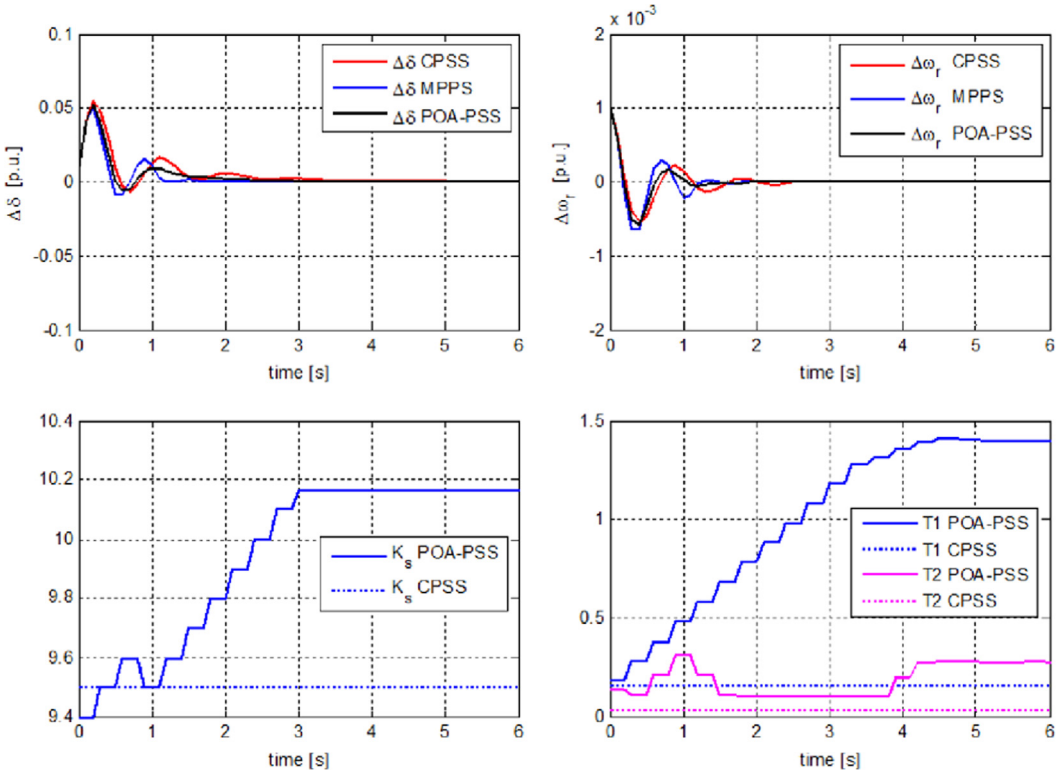

Fig. 6. $\Delta\delta$ and $\Delta\omega_r$ parameters, two circuit connected, P=0.9 pu and Q=0.3 pu.

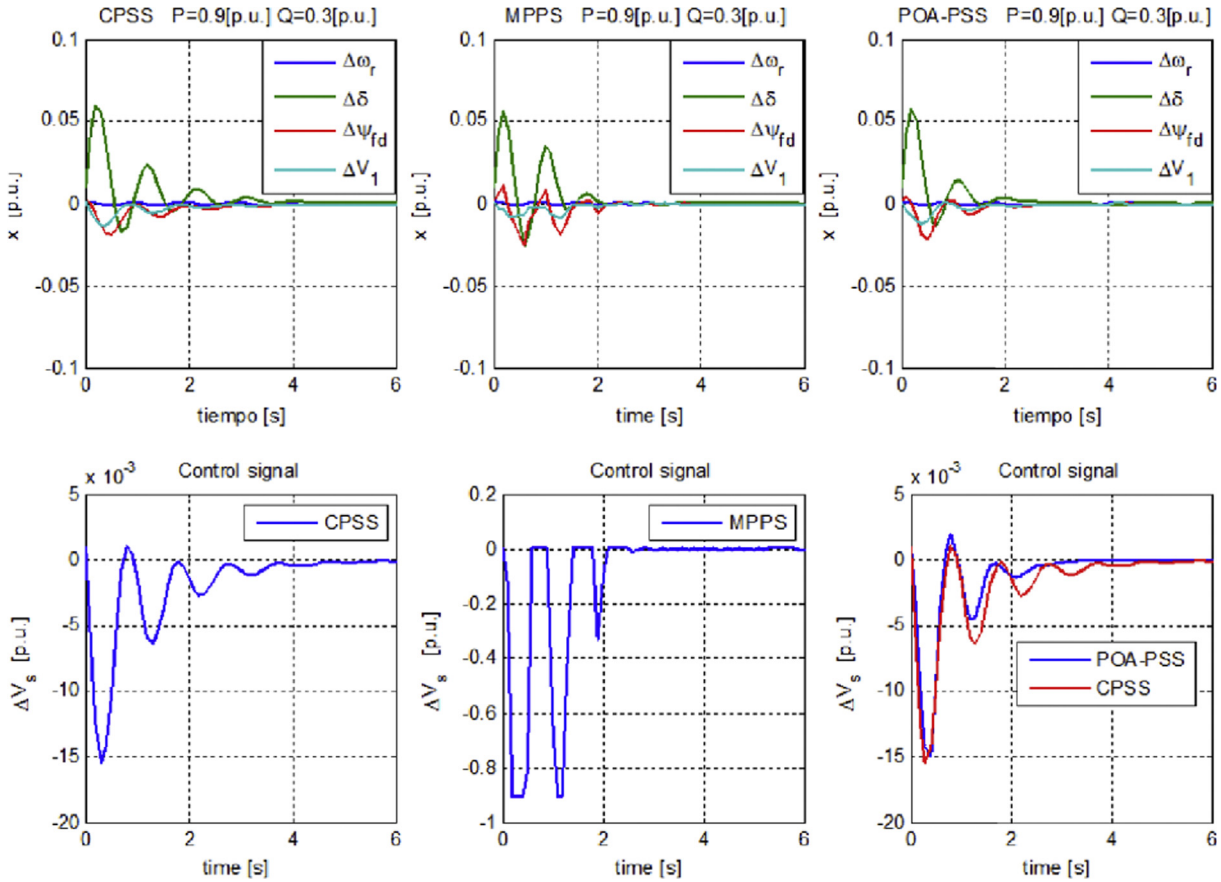

Fig. 7. State and control signal, fall of the second circuit, P=0.9 pu and Q=0.3 pu.

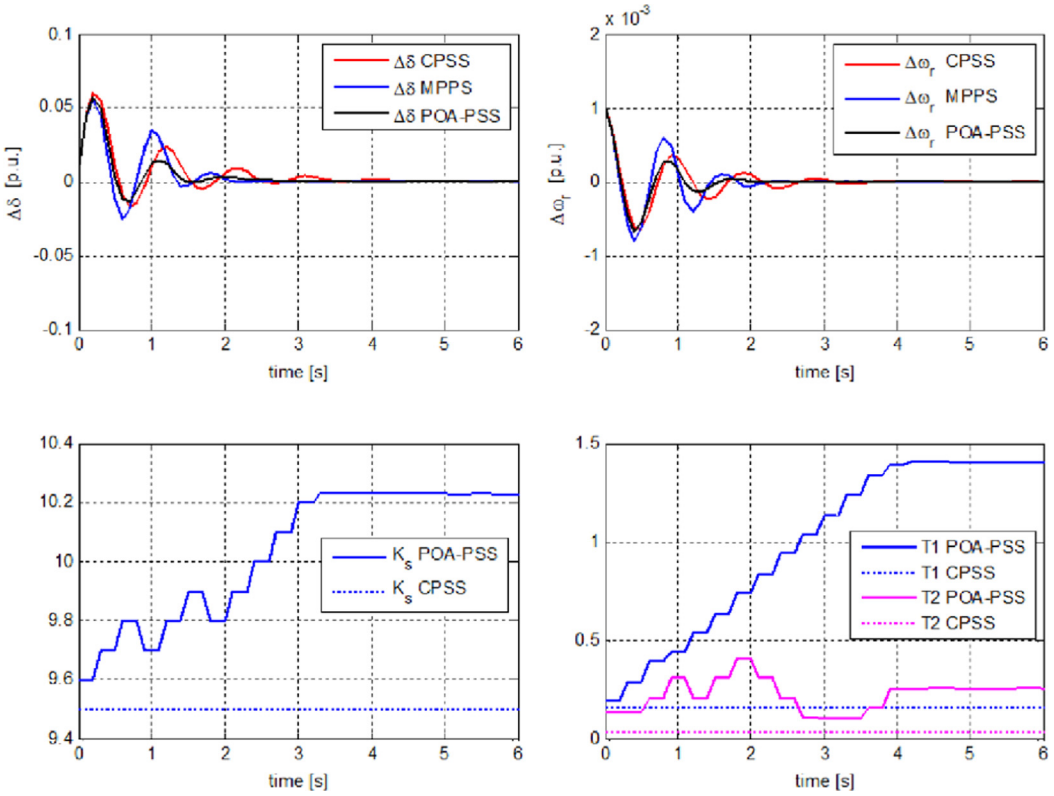

Fig. 8. $\Delta\delta$ and $\Delta\omega_r$ parameters, fall of the second circuit, P=0.9 pu and Q=0.3 pu.

$$\begin{aligned}
&\text{subject to} \quad x(k+1) = A_d(p(k))x(k) + B_d(p(k))\Delta T_m(k)\\
&x(k+2) = A_d(p(k+1))x(k+1) + B_d(p(k+1))\Delta T_m(k+1)\\
&\vdots \qquad\qquad (5)\\
&x(k+N) = A_d(p(k+N-1))x(k+N-1) + B_d(p(k+N-1))\Delta T_m(k+N-1)\\
&\Delta p(k) = p(k) - p(k-1)\\
&\Delta p(k+1) = p(k+1) - p(k)\\
&\vdots\\
&\Delta p(k+N-1) = p(k+N-1) - p(k+N-2) + \text{Constraints of variables}
\end{aligned}$$

where M_a and M_b are weights diagonal matrices belonging to $M_{6\times6}$ and $M_{3\times3}$, respectively.

The solution of the problem described above is achieved by Sequential Quadratic Programming (SQP) algorithm of MATLAB, such that the sampling time does not exceed the time of calculation of the control action, that is 0.3 s. Besides, parameters matrix H_1 and H_2 are obtained by an optimization process with the PSO algorithm, whose mathematical basis can be found in [16].

Stability and robustness analysis has been performed only by experimental evidence and mathematical proof is left as future work.

4. Practical application

In this section, we present the features of the damping strategies used for comparing CPSS and MPPS optimized by PSO [24], the features of the proposed design (POA-PSS), and the evaluation parameters (i.e. settling time and objective function). Finally, the results of the variation of the active power, reactive power and results compared with those presented in reference [13] are presented. In [24], MPPS is proposed to improve the oscillations in a SMIB power system. This approach is part of a small signal stability analysis, which uses equations in an incremental form around an operating point. The MPPS provided the optimal control inputs and design parameters were optimized using particle swarm optimization (PSO). A Classic Power System Stabilizer (CPSS), with parameters also optimized with PSO, was used for comparison.

Table 1
Parameters CPSS.

P (p.u.)	K_s	T_1	T_2
0.5	10.20	0.174	0.0550
0.6	10.01	0.184	0.0450
0.7	9.96	0.177	0.0421
0.8	9.78	0.199	0.0398
0.9	9.46	0.156	0.0342
1.0	9.77	0.166	0.0330

4.1. Features of the damping strategies used for comparison (CPSS, MPPS)

To make a fair comparison with a system whose action control is achieved as a solution of a problem optimization, such as MPPS and POA-PSS, optimal parameters were determined for the CPSS, in this case, K_s, T_1 and T_2 for different active power P. To achieve the parameters, the PSO algorithm was used, with the objective function (6); this function penalizes the signal state $x(t)$, restricted to four main variables of the system $x(t)=[\Delta\omega_r\ \Delta\delta\ \Delta\psi_{fd}\ \Delta V_1]'$, in the simulation time T_f=20 s. Due to the objective function, the state x converges to the origin in minimum time, in addition to requiring that the control signal has minimal variation [19]:

$$\underset{K_s,T_1,T_2}{\text{minimize}}\ J(P) = \sum_{j=1}^{T_f} x(k+j)'Rx(k+j) + \lambda\Delta V_s(k+j-1)^2 \qquad (6)$$

Table 2
Summary simulations, variation in active power P, two circuits connected (E_b=0.995∠0°, Q=0.3 pu, X_e=0.4752 pu).

P (p.u.)	E_t (pu)	O.F. J			$Ts_{\Delta\delta}$		
		CPSS $\times 10^{16}$	MPPS $\times 10^{15}$	POA-PSS $\times 10^{15}$	CPSS (s)	MPPS (s)	POA-PSS (s)
0.5	1∠13.8°	1.35	9.54	6.96	5.90	2.00	3.00
0.6	1∠16.6°	1.20	8.06	6.93	5.90	1.90	3.80
0.7	1∠19.5°	1.09	7.11	6.89	6.00	1.80	3.20
0.8	1∠22.5°	1.01	6.43	6.93	6.10	1.80	3.50
0.9	1∠25.5°	0.94	6.33	7.02	6.10	1.70	3.30
1.0	1∠28.5°	0.89	6.45	7.15	6.00	1.70	3.30
	Means	1.08	6.45	6.98	6.00	1.82	3.35
	Desv. %	15.9	17.3	1.3	1.5	6.4	8.1
	% Improvement w.r.t. CPSS		$I_{J.MPPS}$ 40.27	$I_{J.POA-PSS}$ 35.37		$I_{\delta.MPPS}$ 69.6	$I_{\delta.POA-PSS}$ 44.16

Table 3
Summary simulations, variation in active power P, fall of the second circuit (E_b=0.995∠0°, Q=0.3 pu, X_e=0.65 pu).

P (p.u.)	E_t (pu)	O.F. J			$Ts_{\Delta\delta}$		
		CPSS $\times 10^{16}$	MPPS $\times 10^{15}$	POA-PSS $\times 10^{15}$	CPSS (s)	MPPS (s)	POA-PSS (s)
0.5	1∠19.1°	1.81	1.44	9.86	7.10	2.40	3.70
0.6	1∠23.1°	1.58	1.22	9.86	6.00	2.20	4.50
0.7	1∠27.2°	1.43	1.10	9.42	5.80	2.10	3.30
0.8	1 ∠31.5°	1.30	1.05	9.45	6.30	2.00	3.40
0.9	1∠36°	1.25	1.16	9.42	6.20	2.10	3.30
1.0	1∠40.8°	1.23	1.18	9.55	6.00	2.00	2.90
	Means	1.43	1.19	9.59	6.23	2.13	3.51
	Desv. %	15.8	11.4	2.2	7.4	7.1	15.5
	% Improvement w.r.t. CPSS		$I_{J.MPPS}$ 16.78	$I_{J.POA-PSS}$ 32.93		$I_{\delta.MPPS}$ 65.81	$I_{\delta.POA-PSS}$ 43.65

The parameters optimized with PSO for MPPS [24] are:

$$R=\begin{bmatrix} 3.1\times10^{13} & 0 & 0 & 0 \\ 0 & 5.2\times10^{15} & 0 & 0 \\ 0 & 0 & 7.2\times10^{1} & 0 \\ 0 & 0 & 0 & 9\times10^{3} \end{bmatrix} \quad (7)$$

and $\lambda = 2.1\times10^{5}$.

The parameters optimized with PSO for the CPSS are:

4.2. Features of the proposed POA-PSS design

The results obtained for damping the oscillation modes in SMIB are presented. All tests regarded SMIB initially out of the equilibrium point (in our case the origin), with initial condition $x(0)$= [0.001 0.01 0.001 0.001 0.001 0.001]'. In all tests, the parameters of the objective function (5), the optimization problem of POA-PSS, were constants, i.e. a single predictive controller is used for all comparative tests.

The parameters optimized with PSO for POA-PSS are:

$$M_a=\begin{bmatrix} 1.3\times10^{10} & 0 & 0 & 0 & 0 & 0 \\ 0 & 4.6\times10^{10} & 0 & 0 & 0 & 0 \\ 0 & 0 & 4.1\times10^{5} & 0 & 0 & 0 \\ 0 & 0 & 0 & 8.3\times10^{4} & 0 & 0 \\ 0 & 0 & 0 & 0 & 9.0\times10^{3} & 0 \\ 0 & 0 & 0 & 0 & 0 & 3\times10^{0} \end{bmatrix}$$

and

$$M_b=\begin{bmatrix} 1.1\times10^{1} & 0 & 0 \\ 0 & 1.3\times10^{1} & 0 \\ 0 & 0 & 5.3\times10^{1} \end{bmatrix}$$

Note that the higher parameter is one that penalizes the change in angle $\Delta\delta$.

4.3. Behavioral indices (the settling time and the objective function)

The settling time is a very important measure of power swings in control devices. Damping the system disturbances in the shortest time avoids further damage to the power system. Although the objective (5) function does not include the settling time explicitly, this index is used to compare the classic control strategies CPSS, MPPS [24] and the strategy designed in the current job POA-PSS.

The squared evaluation of the main signals $\Delta\omega_r$, $\Delta\delta$, $\Delta\psi_{fd}$ and ΔV_1 weighted by the diagonal of R in (7), measured in a time of 20 s, has more information than a simple overshoot. Note that the weight of each of them is performed with respect to the parameters obtained in the optimization function in [24], parameters as in (5) and with M_a highlighting the influence of these variables $\Delta\delta$ and $\Delta\omega_r$.

There are a set of 5 tables that present the results of the compared controllers. Results for different active power P and reactive power Q are presented. Results for 1 or 2 connecting transmission circuits are shown, represented by the equivalent impedance X_e and the SMIB transmission voltage E_t. Value of the objective function (5) for CPSS, MPPS and POA-PSS in a range of 20 s is included, and the percent improvement between CPSS and MPPS or POA-PSS, defined as:

$$I_{J\_MPPS}=\frac{(OF_{\_J\_CPSS}-OF_{\_J\_MPPS})\times 100}{OF_{\_J\_CPSS}}$$

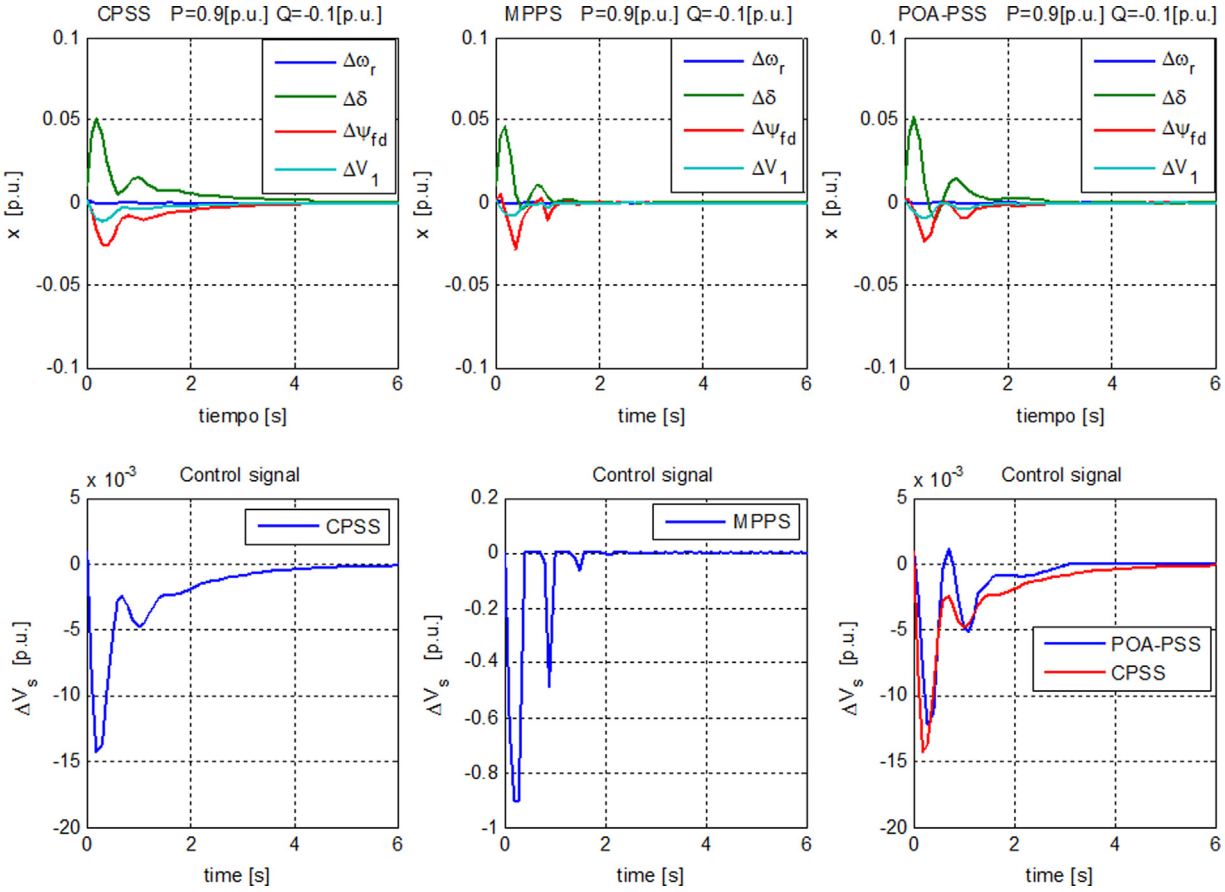

Fig. 9. State and control signal, two circuit connected, $P=0.9$ pu and $Q=-0.1$ pu.

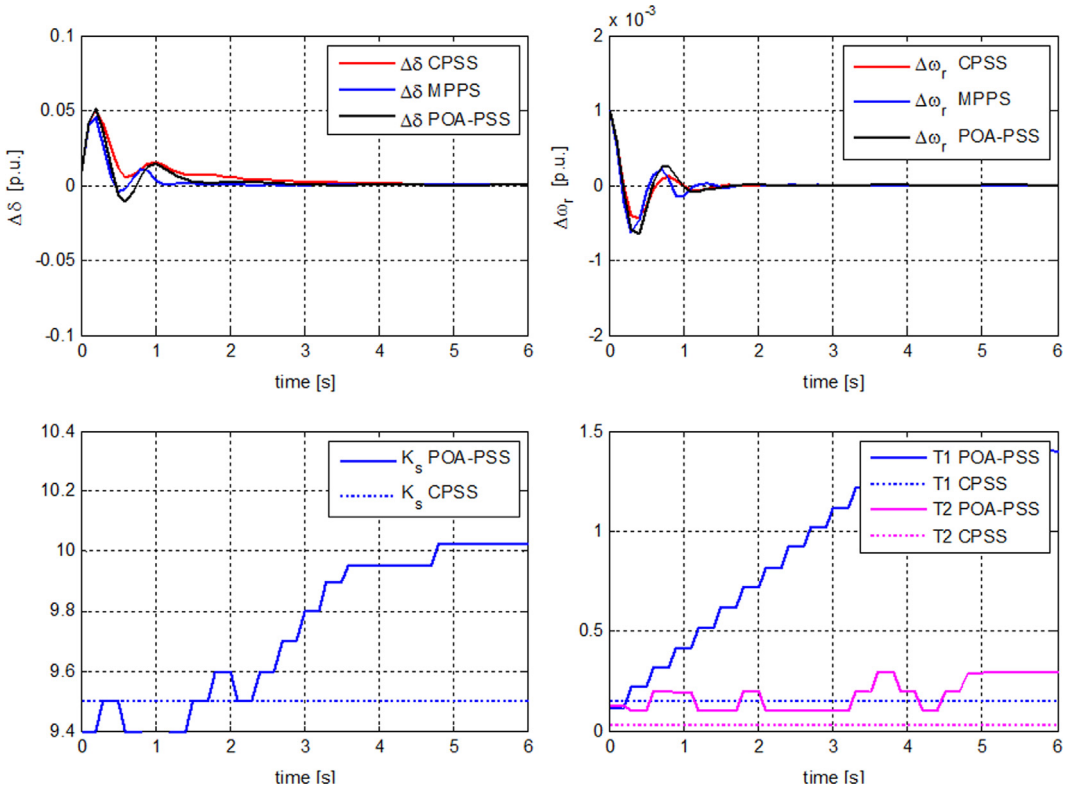

Fig. 10. $\Delta\delta$ and $\Delta\omega_r$ parameters, two circuit connected, $P=0.9$ pu and $Q=-0.1$ pu.

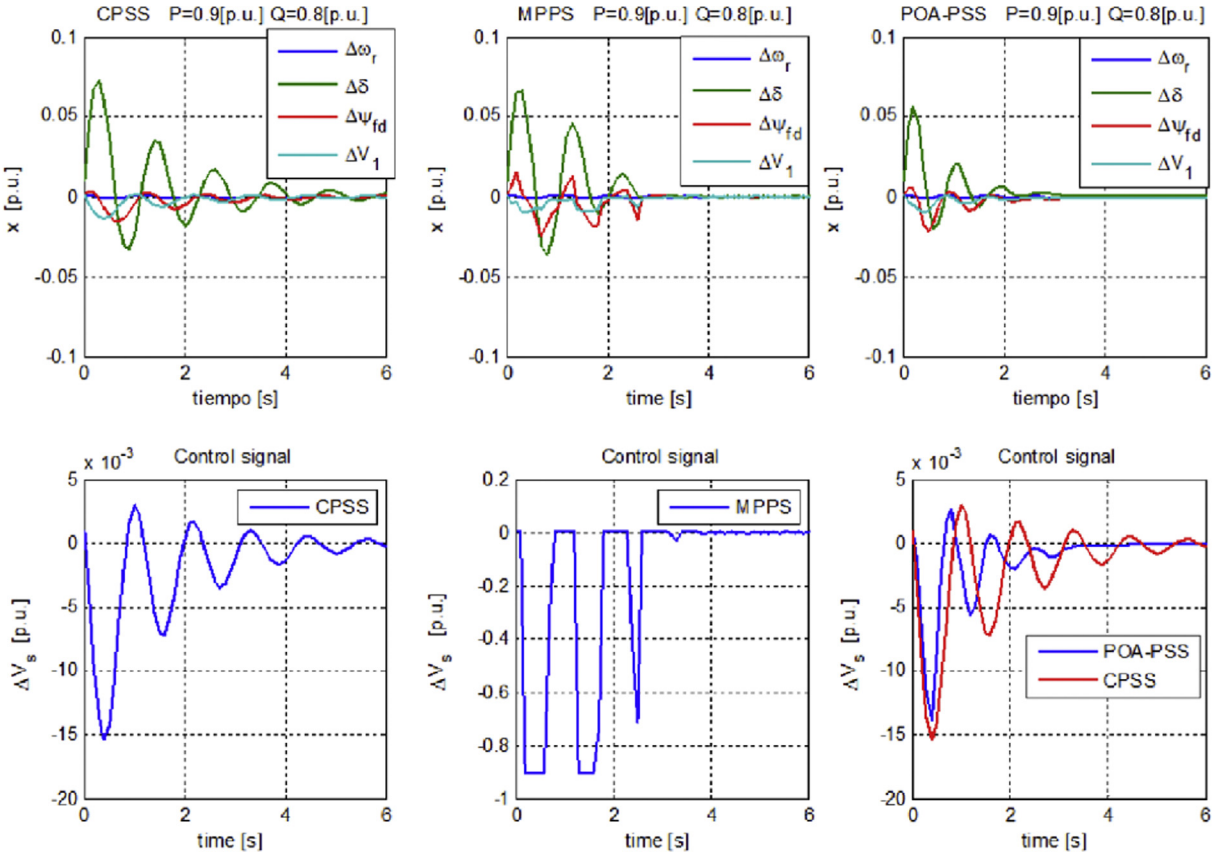

Fig. 11. State and control signal, fall of the second circuit, P=0.9 pu and Q=0.8 pu.

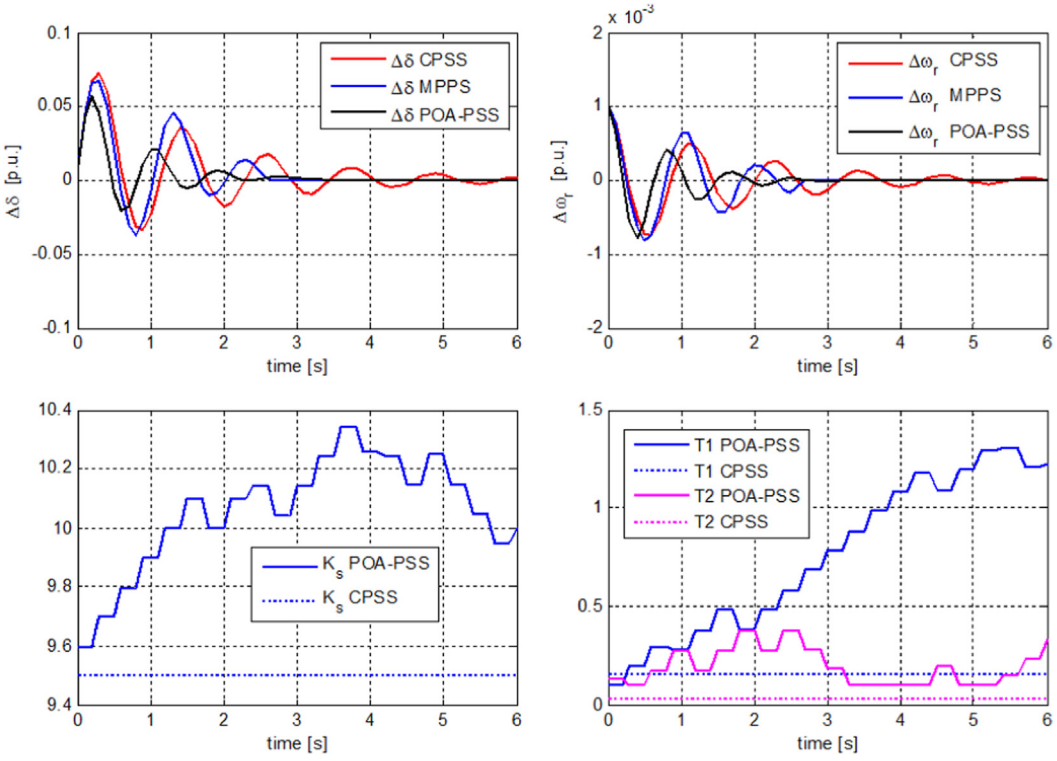

Fig. 12. $\Delta\delta$ and $\Delta\omega_r$ parameters, fall of the second circuit, P=0.9 pu and Q=0.8 pu.

Table 4
Summary simulations, variation in reactive power Q, two circuits connected (E_b=0.995∠0° , P=0.9 pu, X_e=0.4752 pu).

Q (p.u.)	E_t (p.u.)	O.F. J			$Ts_{\Delta\delta}$		
		CPSS $\times 10^{16}$	MPPS $\times 10^{15}$	POA-PSS $\times 10^{15}$	CPSS (s)	MPPS (s)	POA-PSS (s)
0.2	1∠25.5°	0.91	5.99	6.99	6.10	1.70	3.30
0.3	1∠25.5°	0.94	6.33	7.02	6.10	1.70	3.30
0.4	1∠25.5°	0.98	6.79	7.06	6.00	1.80	3.40
0.5	1∠25.5°	1.04	7.45	7.09	6.00	1.90	3.40
0.6	1∠25.5°	1.10	8.29	7.13	6.10	1.90	3.20
0.7	1∠25.5°	1.19	9.10	7.13	6.20	1.90	3.20
0.8	1∠25.5°	0.98	9.88	7.10	6.30	2.00	3.10
−0.1	1∠25.5°	0.83	4.88	6.89	6.30	2.00	3.10
−0.2	1∠25.5°	0.81	4.74	7.08	6.40	1.60	4.10
	Means	0.97	7.04	7.05	6.17	1.83	3.34
	Desv. %	32.7	13.8	1.4	14.7	10.1	12.8
	% Improvement w.r.t. CPSS		$I_{J.MPPS}$ 27.30	$I_{J.POA-PSS}$ 27.30		$I_{\delta.MPPS}$ 70.34	$I_{\delta.POA-PSS}$ 45.86

Table 5
Summary simulations, variation in reactive power Q, fall of the second transmission (E_b=0.995∠0°, P=0.9 pu, X_e=0.65 pu).

Q (p.u.)	E_t (p.u.)	O.F. J			$Ts_{\Delta\delta}$		
		CPSS $\times 10^{16}$	MPPS $\times 10^{15}$	POA-PSS $\times 10^{15}$	CPSS (s)	MPPS (s)	POA-PSS (s)
0.2	1∠36°	1.12	1.07	9.48	6.00	2.50	2.90
0.3	1∠36°	1.12	1.07	9.42	6.00	2.50	3.30
0.4	1∠36°	1.40	1.24	9.39	6.40	2.70	3.40
0.5	1∠36°	1.60	1.43	9.45	6.60	2.20	3.50
0.6	1∠36°	1.85	1.69	9.66	7.70	3.00	3.50
0.7	1∠36°	2.17	1.95	9.69	8.10	2.40	3.50
0.8	1∠36°	2.616	2.39	9.71	8.50	2.40	4.40
	Means	1.69	1.54	9.54	6.29	2.53	3.50
	Desv. %	32.7	31.8	1.4	14.7	10.1	12.8
	% Improvement w.r.t. CPSS		$I_{J.MPPS}$ 8.87	$I_{J.POA-PSS}$ 43.55		$I_{\delta.MPPS}$ 59.77	$I_{\delta.POA-PSS}$ 44.35

and

$$I_{J\_POA-PSS} = \frac{(OF_{\_J\_CPSS} - OF_{\_J\_POA-PSS}) \times 100}{OF_{\_J\_CPSS}}$$

Additionally, the settling time $Ts_{\Delta\delta}$ (for $\Delta\delta$) are shown, together with the corresponding percent of improvement, defined as:

$$I_{\delta\_MPPS} = \frac{(Ts_{\Delta\delta\_CPSS} - Ts_{\Delta\delta\_MPPS}) \times 100}{Ts_{\Delta\delta\_CPSS}}$$

and

$$I_{\delta\_POA-PSS} = \frac{(Ts_{\Delta\delta\_CPSS} - Ts_{\Delta\delta\_POA-PSS}) \times 100}{Ts_{\Delta\delta\_CPSS}}$$

The convergence of $\Delta\delta$ to zero represents the damping of the power oscillation, the main objective of the three controllers compared in this work. In the tables, the settling time is the time elapsed to get and remain within an error band (± 2 %) of the final value.

A set of seven representative figures, with the results of the evolution of the state x of the SMIB, are presented (described by its components $\Delta\omega_r$, $\Delta\delta$, $\Delta\psi_{fd}$ and ΔV_1, and the control action ΔV_s to CPSS, MPPS and POA-PSS).

Representative figures are presented for angle variation $\Delta\delta$, for three controllers, whose convergences are compared in detail; in addition, the frequency variations $\Delta\omega_r$ for three controllers are also detailed. Finally, representative figures, showing the evolution of the variables K_s, T_1 and T_2, are plotted.

4.4. Results obtained by the variation of the active power P

Figs. 5 and 6 show the results with variations in the active power P the connection of the two circuits of the transmission line in the SMIB, with the equivalent impedance X_e=0.4752 pu, which includes the impedance of the two circuits of the transmission line and the impedance of the transformer in this case.

Figs. 7 and 8 show results from fall of the second circuit of transmission line in the SMIB, with the equivalent impedance X_e=0.65 pu, which includes the impedance of the first circuits of the transmission line and the impedance of the transformer in this case.

We can see how the states for the CPSS, MPPS and POA-PSS converge to the origin in all their components at top of Figs. 5 and 7. However, for MPPS and POA-PSS, the convergence is faster than CPSS. The same process occurs for $\Delta\delta$ and $\Delta\omega_r$ at the top of Figs. 6 and 8, i.e. the oscillation is damped faster in the MPPS or POA-PSS than in the CPSS.

The settling time of the MPPS is shorter than that of the POA-PSS; however, the effort in control action of the POA-PSS is much less than that of the MPPS (even less than that of the CPSS), and this is shown at the bottom of Figs. 5 and 7.

At the bottom of Figs. 6 and 8 is shown a transient and permanent regime of K_s, T_1 and T_2 similar to the controlled signal behavior of the $\Delta\delta$ (Table 1).

In Table 2 a summary of simulations, with variations in active power P and two connected circuits is presented. There are, on an average, improvements of 40.27% and 35.37% of the objective

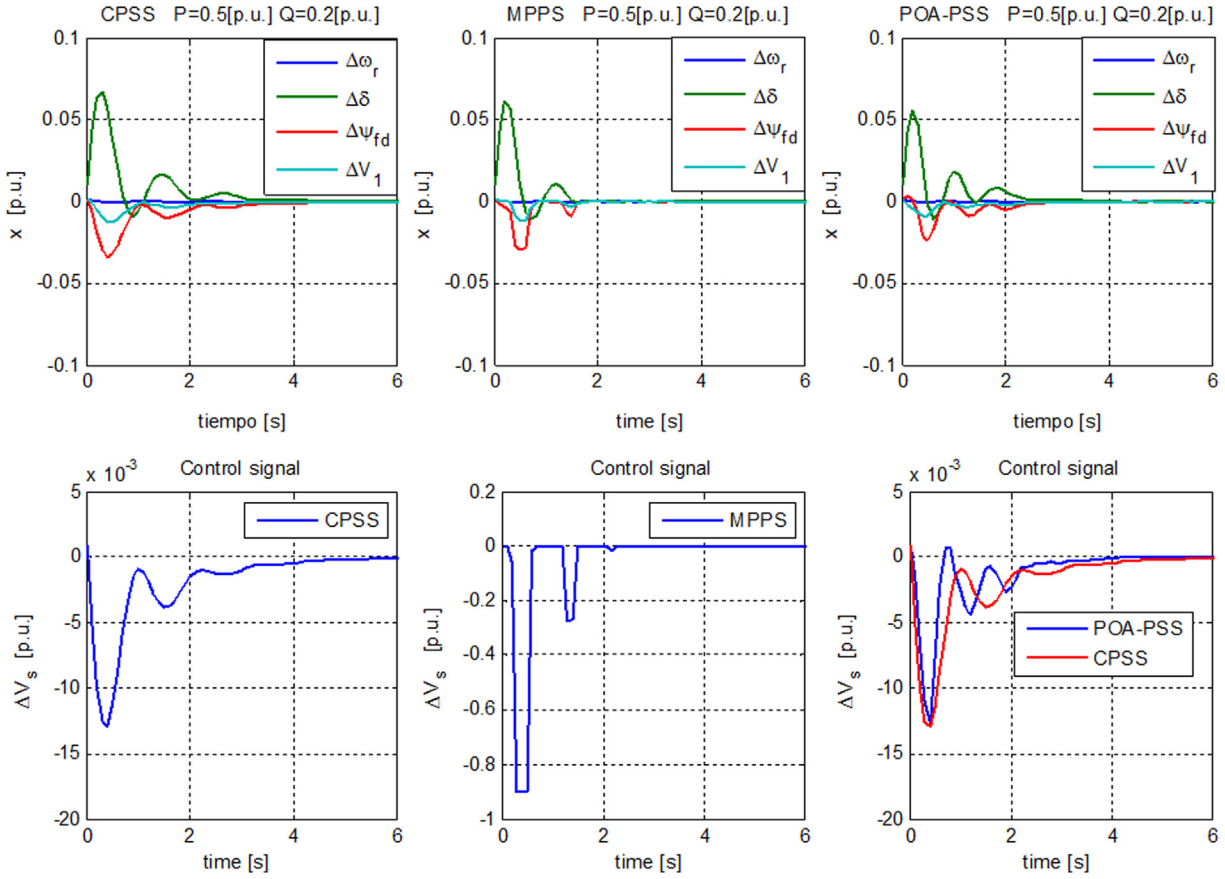

Fig. 13. State and control signal, two circuit connected, P=0.5 pu and Q=0.2 pu.

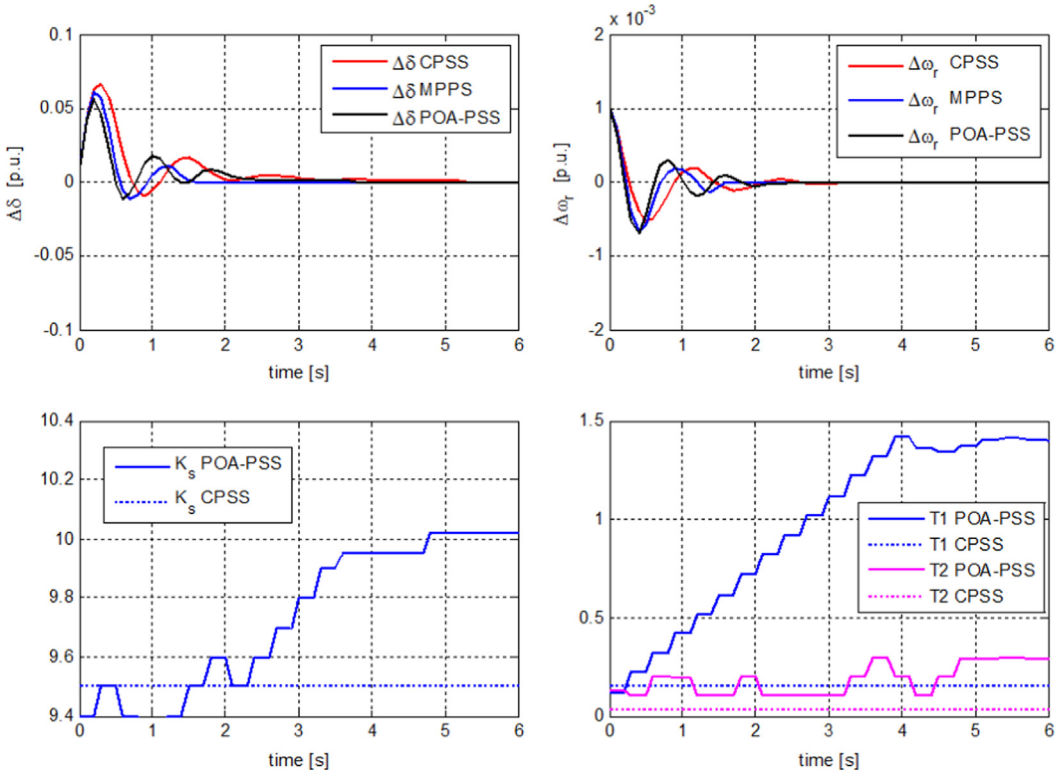

Fig. 14. $\Delta\delta$ and $\Delta\omega_r$ parameters, two circuit connected, P=0.5 pu and Q=0.2 pu.

Table 6
Results of comparison, regarding paper [8] ($E_t = 1\angle 0°$).

P (p.u.)	Q (p.u.)	X_e (p.u.)	O.F. J			$Ts_{\Delta\delta}$		
			CPSS $\times 10^{16}$	MPPS $\times 10^{15}$	POA-PSS $\times 10^{15}$	CPSS (s)	MPPS (s)	POA-PSS (s)
0.2	−0.2	1.0800	3.57	3.09	2.71	10.10	3.10	6.50
0.5	0.2	0.4752	1.71	1.10	8.94	6.30	2.10	3.90
		Means	2.64	2.10	5.82	8.2	2.6	5.2
		% Improvement w.r.t. CPSS		$I_{J.MPPS}$ 20.45	$I_{J.POA-PSS}$ 77.95		$I_{\delta.MPPS}$ 68.29	$I_{\delta.POA-PSS}$ 36.58

Table 7
Comparison of MPPS and POA-PSS objective functions.

Means OF J MPPS $\times 10^{15}$	Desv. % MPPS	Means OF J POA-PSS $\times 10^{15}$	Desv. % POA-PSS	Table
6.45	17.3	6.98	1.3	2
11.9	11.4	9.59	2.2	3
7.04	13.8	7.05	1.4	4
15.4	31.8	9.54	1.4	5

function (O.F.) of the MPPS and POA-PSS respectively, compared with CPSS. Similarly, there are an average improvement of 69.70% and 44.16% of the settling time of the MPPS and POA-PSS respectively, in comparison with CPSS.

In Table 3, a summary of simulations with variations in active power P, for fall of the second circuit of the transmission line, is presented. There is an average improvement of 16.78% and 32.93% of the objective function (O.F.) of the MPPS and POA-PSS respectively, compared with CPSS. Similarly, there is an average improvement of 65.81% and 43.65% of the settling time of $\Delta\delta$ the MPPS and POA-PSS respectively, compared to CPSS.

4.5. Results obtained by the variation in reactive power Q

In Figs. 9 and 10, the results with variations reactive power Q the connection of the two circuits of the transmission line in the SMIB are shown. Figs. 11 and 12 show results from fall of the second circuit of transmission line in the SMIB. We can see how the states for the CPSS, MPPS and POA-PSS converge to the origin in all their components at the top of Figs. 9 and 11. However, for MPPS and POA-PSS, the convergence is faster than CPSS. Same process occurs for $\Delta\delta$ and $\Delta\omega_r$ in the top of Figs. 10 and 12, i.e. the oscillation is damped faster in MPPS or POA-PSS than in CPSS. The effort in control action of the POA-PSS is much less than of the MPPS (even less than of the CPSS), which is shown at the bottom of Figs. 9 and 11. A transient and permanent regime of K_s, T_1 and T_2 similar to the controlled signal behavior is shown at the bottom of Figs. 10 and 12.

In Table 4 a summary of simulations with variations reactive power Q and two connected circuits is presented. There is an equal average improvement of 27.30% of the objective function (OF) of the MPPS and POA-PSS, compared with CPSS. However, the values of the OF are equal, the value of the objective function (OF) of the POA-PSS is more accurate because it has less dispersion.

In Table 4, there is an average improvement of 70.34% and 45.86% of the settling time of $\Delta\delta$ the MPPS and POA-PSS respectively, in comparison with CPSS.

In Table 5 a summary of simulation is presented with variations in reactive power Q with fall of the second circuit of the transmission line. There are an average improvement of 8.87% and 43.55% of the objective function (OF) of the MPPS and POA-PSS, respectively, compared with CPSS. Note again that the value of the objective function of the POA-PSS is more accurate because it has less dispersion. In Table 5, there are an average improvement of 59.77% and 44.35% of the settling time of $\Delta\delta$ the MPPS and POA-PSS respectively, in comparison with CPSS.

4.6. Comparative results with those in reference [13]

In Figs. 13 and 14, comparative results with paper [13] with fall of the first circuit of transmission line and with the connection of the two circuits in the SMIB are shown. We can see at the top of Fig. 13 how the states for the CPSS, MPPS and POA-PSS converge to the origin in all their components. The signals $\Delta\delta$ of MPPS and POA-PSS converge faster than the signals of the CPSS, the same happens for the $\Delta\omega_r$.

The effort in control action of the POA-PSS is much less than of the MPPS (even less than of the CPSS), this is shown at the bottom of Fig. 13. A transient and permanent regime of K_s, T_1 and T_2, similar to the controlled signal $\Delta\delta$ behavior is shown at the bottom of Fig. 15.

In Table 6, results comparable to paper [13] during the fall of the first circuit of transmission line and during the connection of the two circuits are presented. There are an average improvement of 20.45% and 77.95% of the objective function (OF) of the MPPS and of the POA-PSS, with respect to CPSS. Similarly, there are an average improvement of 68.29% and 36.58% of the settling time of the MPPS, with respect to CPSS.

In general, POA-PSS achieves a 44.5% improvement in settling time compared to a traditional CPSS control (see Tables 2–7), which can be considered to be an interesting improvement. This result is not better than the 66.4% improvement obtained by MPPS (see Tables 2–7). However, MPPS requires a control effort of two orders of magnitude larger as compared with POA-PSS (see Figs. 5, 7, 9, 11 and 13). Besides, in MPSS at the beginning the voltage Vs decreases about 80% which could cause instability of the power system under certain conditions (see Figs. 5, 7, 9, 11 and 13).

Table 7 presents a comparison between MPPS and POA-PSS methods according to the objective function using the average information (mean and standard deviation) from Tables 2 to 5, that can be considered to be representative of the overall behavior of each method. We can see from Table 7 that the average of MPPS is marginally better than POA-PSS for the operating conditions represented in Tables 2 and 4. Instead, for the operating conditions presented in Tables 3 and 5, POA-PSS is distinctively better than MPPS. Besides, the statistical deviations of the POA-PSS are an order of magnitude less than those of MPPS in all the cases studied, indicating that POA-PSS behavior is more reliable.

Finally, because we work with small signal models, variations less than 1% were selected for the parameter of interest, which produces power oscillations $\Delta\delta$. Overall system response is proportional to the change of the initial condition. Variations on other elements of the state vector $x(t) = [\Delta\omega_r\ \Delta\delta\ \Delta\psi_{fd}\ \Delta V_1\ \Delta V_2\ \Delta V_s]'$ should be analyzed in future studies for instance, variations should

be compared with a primary frequency control of the EPS [17] controller, not included in the diagram of Fig. 2.

5. Conclusions

PSS devices are responsible for providing a damping torque component to generators; for reducing fluctuations in the system caused by small perturbations. In this paper a Predictive Optimized Adaptive PSS (POA-PSS) to improve the oscillations, in a single machine infinite bus (SMIB) power system, is considered. POA-PSS provides optimal design parameters K_s, T_1 and T_2 of classic PSS using an optimization predictive algorithm, which adapts to changes in the inputs to the system.

A CPSS, with parameters optimized with PSO, and an MPPS were used for comparison. Simulation studies on the SMIB power system illustrate that the proposed POA-PSS and MPPS approach have better performance than the classical PSS for all the powers and changes the parameters of the system considered. Nevertheless, the effort in control action of the POA-PSS is much less than that of the MPPS and even less than that of the CPSS.

The statistical deviation of the POA-PSS is an order of magnitude less than the MPPS, and therefore the behavior of the POA-PSS is more reliable.

As future work, we propose to implement the POA-PSS algorithm in a system of multiple connected generators and adapt the goal of every controller to centralized decision functions.

Acknowledgments

The results reported in this paper have been financed by CONICYT-Chile, under the Basal Financing Program FB0809 “Advanced Mining Technology Center”. The first author would like to thank the support of FONDECYT 3140604, “Postdoctoral”.

References

[1] Ramírez-Arredondo JM. The closed-loop characteristic polynomial as a means to obtain robust performance of conventional PSS. Electr Power Energy Syst 2000;22:259–68.
[2] Anderson PM. Power system dynamics and stability. Ames, IA: Iowa State University Press; 1977.
[3] Concordia C, de Mello FP. Concepts of synchronous machine stability as affected by excitation control. IEEE Trans Power Appar Syst 1969;PAS-88:316–29.
[4] Sauer PW, Pai MA. Power system dynamics and stability. Englewood, Cliffs, NJ, USA: Prentice-Hall; 1998.
[5] Stativ A, Gavrila M. Optimal tuning and placement of power systemstabilizer using particle swarm optimization. In: Algorithm2012 International conference and exposition on electrical and power engineering, Iasi, Romania, 2012. p. 25–7.
[6] Karnik SR, Raju AB, Raviprakasha MS. Robust design of power system stabilizer using taguchi technique and particle swarm optimization. In: Second international conference on emerging trends in engineering and technology, vol. 1, No. 1, 2009. p. 19–25.
[7] Kahl M, Leibfried T. Decentralized model predictive control of electrical power systems. In: Conference on power systems transients (IPST2013), Vancouver, Canada, July 2013. p. 18–20.
[8] Shoiib-Shahriar Md, Ashik-Ahmed Md, Shahid-Ullah Md. Design and analysis of a model predictive unified power flow controller (MPUPFC) for power system stability assessment. Int J Electr Comput Sci IJECS-IJENS 12(04);2012.
[9] Phulpin Y, Hazra, J, Ernst, D. Model predictive control of HVDC power flow to improve transient stability in power systems. In IEEE international conference on smart grid communications (SmartGridComm), 2011. p. 593–8.
[10] Sebaa K, Moulahoum S, Houassine H, Kabache N. Model predictive control to improve the power system stability. In 13th international conference on optimization of electrical and electronic equipment (OPTIM), 2011. p. 208–12.
[11] Ford JJ, Ledwich G, Dong ZY. Efficient and robust model predictive control for first swing transient stability of power systems using flexible AC transmission systems devices. Gener Transm Distrib 2008;2(5):731–42.
[12] Rajkumar V, Mohler RR. Nonlinear predictive control for the damping of multimachine power system transients using FACTS devices. In Proceedings of the 33rd conference on decision and control, Lake Buena Vista, vol. 4, December 1994. p. 4074–9.
[13] Chatterjee A, Ghoshal SP, Mukherjee V. Chaotic ant swarm optimization for fuzzy-based tuning of power system stabilizer. Electr Power Energy Syst 2011;33:657–72.
[14] Camacho EF, Bordons C. Model predictive control. London: Springer-Verlag; 1999.
[15] Mayne DQ, Rawlings JB, Rao CV, Scokaert POM. Constrained model predictive control: stability and optimality. Automatica 2000;36:789–814.
[16] Kennedy J, Eberhart RC. Swarm intelligence. San Francisco: Morgan Kaufmann; 2001.
[17] Kundur P. Power system stability and control. New York: McGraw-Hill; 1994.
[18] Wang L, Cheung H, Hamlyn A, Cheung R. Model prediction adaptive control of inter-area oscillations in multi-generators power systems. In: Power and energy society general meeting, Toronto, Canada, 2009. p. 1–7.
[19] Abido MA. Optimal design of power-system stabilizers using particle swarm optimization. IEEE Trans Energy Convers 2002;17(3):406–13.
[20] Mahmoodi E, Farsangi MM. Design of stabilizing signals by using model predictive control. Int J Tech Phys Probl Eng 2010;2:1–4.
[21] Jain A, Biyik E, Chakrabortty A. A model predictive control design for selective modal damping in power systems. In: Proceedings of the American control conference, Chicago, July 2015. p. 4314–9.
[22] Yousef AM. Neural network predictive control based power system stabilizer. J Eng Sci 2011;39(6):1431–47.
[23] Zahran M, Yousef AM, Moustafa G. Design of model predictive control for adaptive damping of power system stabilization. WSEAS Trans Syst Control 2015;10:685–94.
[24] Duarte-Mermoud MA, Milla F. Model predictive power stabilizer optimized by PSO. J Electr Power Syst., submitted for publication, 2016. Unpublished results.